

Contact Self-Cleaning of Synthetic Gecko Adhesive from Polymer Microfibers

Jongho Lee^{*,†} and Ronald S. Fearing[‡]

Department of Mechanical Engineering and Department of Electrical Engineering and Computer Sciences, University of California, Berkeley, California 94720

Received July 7, 2008. Revised Manuscript Received August 21, 2008

Natural gecko toes covered by nanomicro structures can repeatedly adhere to surfaces without collecting dirt. Inspired by geckos, we fabricated a high-aspect-ratio fibrillar adhesive from a stiff polymer and demonstrated self-cleaning of the adhesive during contact with a surface. In contrast to a conventional pressure-sensitive adhesive (PSA), the contaminated synthetic fibrillar adhesive recovered about 33% of the shear adhesion of clean samples after multiple contacts with a clean, dry surface.

Conventional pressure-sensitive adhesives (PSA) use soft viscoelastic polymers (Young's modulus < 100 kPa measured at 1 Hz^{-1-3}) to make intimate contact with surfaces to achieve high adhesion. However, soft polymers tend to collect dirt and lose adhesion with repeated use. In contrast, a gecko uses millions of keratinous nano and microhairs (Young's modulus $E \approx 1.5$ GPa^{3,4}) to cling to and walk on virtually any surface. These hairs shed dirt particles during contact with a surface, keeping its natural adhesive sufficiently clean to support the gecko's body weight.⁵

A key factor in the self-cleaning ability of gecko structures is the nonadhesive default state exhibited by the gecko fibers.⁶ To adhere, the fibers need to be dragged to expose the spatula tips, increasing the contact fraction by approximately 7.5-fold.⁶ In contrast to the well-known lotus effect⁷ in which particles are removed from a nonadhesive and highly hydrophobic surface by water droplets, gecko setae self-clean particles during use, even on dry surfaces. We restrict our discussion here to the self-cleaning of adhesives on dry surfaces during use. Natural gecko setae are the only previously reported self-cleaning adhesive on dry surfaces.

Recently, gecko-inspired synthetic adhesives (GSAs)⁸ have been fabricated using soft polymers (Young's modulus ≤ 10 MPa)^{9–14} or hard polymers^{15–18} (Young's modulus ≥ 1.5 GPa). Also, arrays of carbon nanotubes (CNT) have been used to achieve

adhesion.^{19–21} Fibrillar adhesive cleaning has been demonstrated using water^{16,22} and mechanical vibration.²² Superhydrophobicity may lead to the cleaning of fibrillar adhesive by water.²³ However, no synthetic adhesive has demonstrated self-cleaning on dry surfaces during use, one of the important advantages of a gecko-inspired adhesive over conventional pressure-sensitive adhesives.

Autumn²⁴ has identified seven benchmark properties that are characteristic of geckolike adhesives, which are (1) anisotropic attachment, (2) a high adhesion coefficient, (3) a low detachment force, (4) material-independent adhesion, (5) self-cleaning, (6) anti-self-adhesion, and (7) a nonsticky default state. Although properties 1–4 and 7 have been previously demonstrated^{25,26} in a single material, in this letter we report the first geckolike microfibrillar material that also demonstrates self-cleaning during contact.

To create a self-cleanable adhesive, we fabricated high-aspect-ratio fibrillar arrays from polypropylene (Young's modulus $E \approx 1.5$ GPa, measured with Sintech tensile tester 2/S, MTS Systems). In previous work, these hard-polymer-based fibrillar materials have shown unique adhesion properties, similar to those of gecko setae, including sliding enhanced shear adhesion²⁵ with low peeling force and frictional adhesion²⁷ with a spherical indenter.²⁸ In this letter, we use a contact "step" protocol similar to that used for natural gecko setal arrays⁵ to demonstrate self-cleaning of the synthetic fibrillar adhesive. The self-cleaning synthetic

* To whom correspondence should be addressed. E-mail: jongho@eecs.berkeley.edu.

[†] Department of Mechanical Engineering.

[‡] Department of Electrical Engineering and Computer Sciences.

(1) Dahlquist, C. A. In *Treatise on Adhesion and Adhesives*; Patrick, R. L. Ed.; Dekker: New York, 1969.

(2) Pocius, A. V. *Adhesion and Adhesive Technology*, Hanser: Munich, 2002; Chapter 3.

(3) Autumn, K.; Majidi, C.; Groff, R. E.; Dittmore, A.; Fearing, R. J. *Exp. Biol.* **2006**, *209*, 3555.

(4) Peattie, A. M.; Majidi, C.; Corder, A.; Full, R. J. *J. R. Soc. Interface* **2007**, *4*, 1071.

(5) Hansen, W. R.; Autumn, K. *Proc. Natl. Acad. Sci. U.S.A.* **2005**, *102*, 385.

(6) Autumn, K.; Hansen, W. *J. Comp. Physiol., A* **2006**, *192*, 1205.

(7) Barthlott, W.; Neinhuis, C. *Planta* **1997**, *202*, 1.

(8) Autumn, K.; Gravish, N. *Philos. Tran. R. Soc. A* **2008**, *366*, 1575.

(9) Sitti, M.; Fearing, R. S. *J. Adhes. Sci. Technol.* **2003**, *18*, 1055.

(10) Gorb, S.; Varenberg, M.; Peressadko, A.; Tuma, J. J. *J. R. Soc. Interface* **2006**, *4*, 271.

(11) Kim, S.; Sitti, M. *Appl. Phys. Lett.* **2006**, *89*, 261911.

(12) Murphy, M. P.; Aksak, B.; Sitti, M. *J. Adhes. Sci. Technol.* **2007**, *21*, 1281.

(13) Crosby, A. J.; Hageman, M.; Duncan, A. *Langmuir* **2005**, *21*, 11738.

(14) Glassmaker, N. J.; Jagota, A.; Hui, C.-Y.; Noderer, W. L.; Chaudhury, M. K. *Proc. Natl. Acad. Sci. U.S.A.* **2007**, *104*, 10786.

(15) Geim, A. K.; Dubonos, S. V.; Grigorieva, I. V.; Novoselov, K. S.; Zhukov, A. A.; Shapoval, S. Yu. *Nat. Mater.* **2003**, *2*, 461.

(16) Kustandi, T. S.; Samper, V. D.; Yi, D. K.; Ng, W. S.; Neuzil, P.; Sun, W. *Adv. Funct. Mater.* **2007**, *17*, 2211.

(17) Northen, M. T.; Turner, K. L. *Sens. Actuators, A* **2006**, *130*, 583.

(18) Schubert, B.; Majidi, C.; Groff, R. E.; Baek, S.; Bush, B.; Maboudian, R.; Fearing, R. S. *J. Adhes. Sci. Technol.* **2007**, *21*, 1297.

(19) Zhao, Y.; Tong, T.; Delzeit, L.; Kashani, A.; Meyyappan, M.; Majumdar, A. *J. Vac. Sci. Technol., B* **2006**, *24*, 331.

(20) Ge, L.; Sethi, S.; Ci, L.; Ajayan, P. M.; Dhinojwala, A. *Proc. Natl. Acad. Sci. U.S.A.* **2007**, *104*, 10792.

(21) Qu, L.; Dai, L. *Adv. Mater.* **2007**, *19*, 3844.

(22) Sethi, S.; Ge, L.; Ci, L.; Ajayan, P. M.; Dhinojwala, A. *Nano Lett.* **2008**, *8*, 822.

(23) Bhushan, B.; Sayer, R. A. *In Microsys. Technol.* **2007**, *13*, 71.

(24) Autumn, K. In *Biological Adhesives*; Smith, A. M., Callow, J. A., Eds.; Springer Verlag: Berlin, 2006; pp 225–255.

(25) Lee, J.; Majidi, C.; Schubert, B.; Fearing, R. S. *J. R. Soc. Interface* **2008**, *5*, 835.

(26) Kim, S.; Spenko, M.; Trujillo, S.; Heyneman, B.; Santos, D.; Cutkosky, M. R. *IEEE Trans. Robot.* **2008**, *24*, 65.

(27) Autumn, K.; Dittmore, A.; Santos, D.; Spenko, M.; Cutkosky, M. *J. Exp. Biol.* **2006**, *209*, 3569.

(28) Schubert, B.; Lee, J.; Majidi, C.; Fearing, R. S. *J. R. Soc. Interface.* **2008**, *5*, 845.

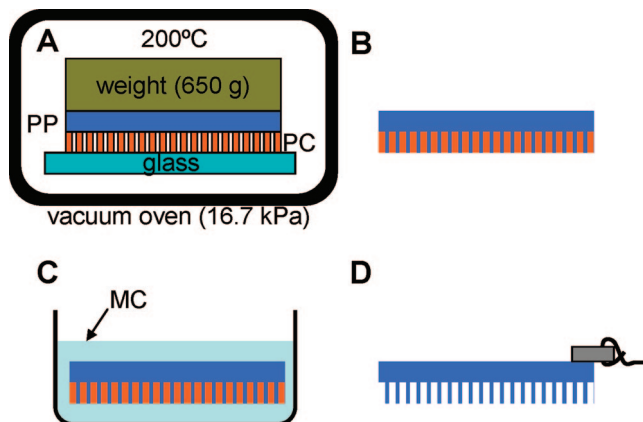


Figure 1. Schematic illustration of the fabrication process of polypropylene fibrillar adhesives. (A) A polypropylene (PP) film was cast into a polycarbonate (PC) template for 28 min in a vacuum oven at 200 °C. (B) The casted PP film and PC template cooled down to room temperature for 30 min. (C) The PC template was etched completely for 10 min in a first bath and 5 min in a second bath of methylene chloride (MC). (D) The resulting sample was rinsed in isopropyl alcohol and air dried. A string-connected load bar was attached to distribute the pulling force evenly.

adhesive should be useful in a variety of applications where conventional adhesives can be easily contaminated.

The fibrillar adhesives were fabricated by casting a single layer of a 25- μm -thick polypropylene (PP) film (TF-225-4, Premier Laboratory Supply Inc.) in a vacuum oven at 200 °C into a 20- μm -thick polycarbonate (PC) track-etched membrane filter (ISOPORE, Millipore Inc.) containing 300-nm-radius pores as illustrated in Figure 1A. Using a fixed fiber length, this fiber radius was selected to provide bending compliance while preventing fibers from clumping. The polycarbonate filter was etched completely for 10 min in a first bath and 5 min in a second bath of methylene chloride (Figure 1C) to release the polypropylene fibrillar surface and film. The resulting samples were rinsed in isopropyl alcohol and air dried (Figure 1D). The polypropylene film contains approximately 42 million fibers per square centimeter with the average length and radius of the fibers being 18 μm and 300 nm, respectively. The microstructured polypropylene film was cut into 2 cm \times 2.5 cm rectangles using a razor blade, and a 2 cm \times 0.5 cm \times 0.05 cm load bar with a small hole in which a string goes through was attached to distribute the pulling force uniformly.

To simulate contamination with dirt particles, microspheres with a mean radius of 1.15 μm (gold powder, spherical, radius $\leq 2.5 \mu\text{m}$, Alfa Aesar) were applied to cover the whole area of fibrillar adhesives and conventional pressure-sensitive adhesives by freely dropping microspheres from about 5 cm above the adhesives. (Au microspheres were supplied in dry powder form with only weak clumping. Au microspheres were applied uniformly with similar density on the PSA and fibrillar surfaces by gravity, without applying any contact force.) After application, the adhesives were gently shaken to remove excess microsphere particles. As shown in Figure 2A,C, microspheres initially covered most of the area.

The samples were tested using a “simulated step” protocol shown in Figure 3 similar to a gecko’s walking step. The samples were first compressively loaded ($< 1 \text{ N/cm}^2$) onto a clean glass substrate manually with a gloved finger (Figure 3A). (It has been shown previously that the shear strength is independent of the initial normal preload.²⁵) The samples were next loaded parallel to the glass substrate by a weight attached to the load bar through a string (Figure 3B), and then the normal load was removed

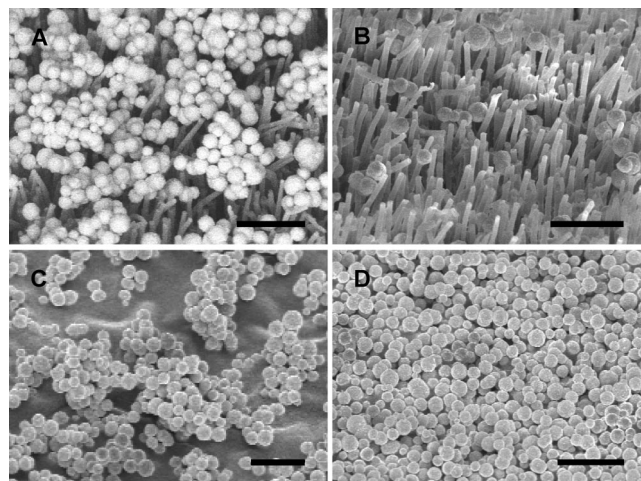


Figure 2. Scanning electron micrograph images of the polypropylene fibrillar adhesive and conventional pressure-sensitive adhesives (PSA). (A) Fibrillar adhesive contaminated by gold microspheres. (B) Fibrillar adhesive after 30 contacts (simulated steps) on clean glass substrate. (C) Conventional PSA contaminated by microspheres. (D) Conventional PSA after contact on a clean glass substrate. All scale bars correspond to 10 μm . Microspheres on fibrillar adhesive are removed by simulated steps, but microspheres on PSA cover more area after the steps.

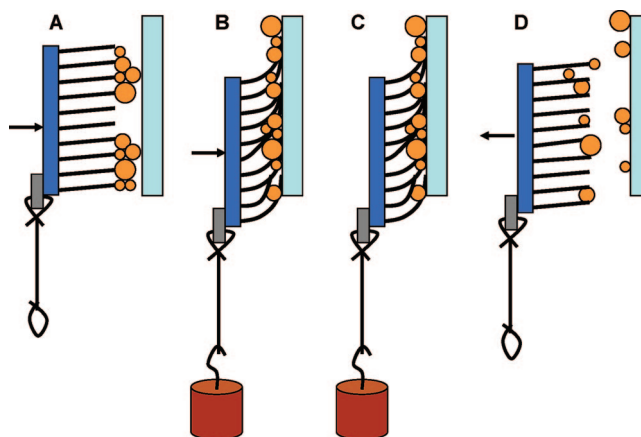


Figure 3. One cycle of simulated steps, with contact with an initially clean glass slide. (A) Applying normal compressive force. (B) Shear load added to the compressive load by a hanging weight. (C) Removing the compressive load (pure shear loading). (D) Detaching the sample.

while maintaining the parallel load (Figure 3C). If the sample could hold the weight, then we removed the sample from the substrate manually (Figure 3D) and increased the weight for the next step. If the sample could not hold the weight, then the sample fell and was caught by a gloved hand just below the weight. In case of failure to support the weight, we used the same weight for the next simulated step. Before each simulated step, the glass substrate was cleaned with isopropyl alcohol to remove residual particles. After 30 simulated steps, the fibrillar adhesive shed about 60% of the microspheres onto the glass substrate as shown in Figure 2B. Some microspheres remained embedded between fibers and were not self-cleaned. As a control, we used a 0.2 cm \times 0.5 cm conventional pressure-sensitive adhesive (PSA) (Scotch Magic Tape, 3M). After the simulated steps, the soft polymer of the conventional PSA was almost completely covered by microspheres, as shown in Figure 2D. This is possibly because microspheres not in direct contact with the soft polymer are taken off and recaptured in the exposed area of the soft polymer during simulated steps.

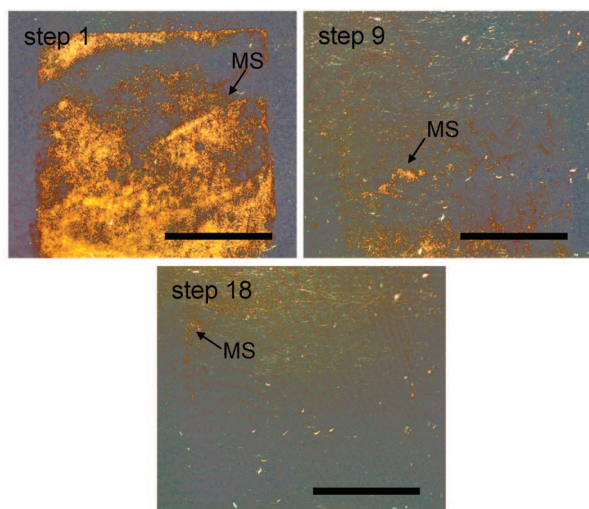
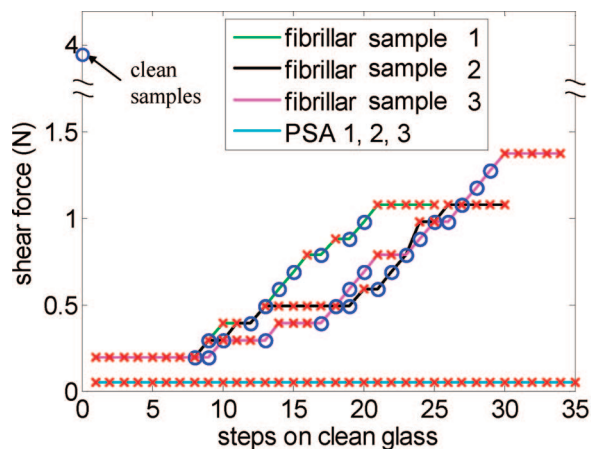


Figure 4. Steps on clean glass and recovered shear adhesion. Clean samples could hold 4 N shear force. Samples contaminated by gold particles (mean radius $1.15 \mu\text{m}$) recovered up to 33% of the shear adhesion of clean samples. (x) Indicates a shear force that could not be sustained by the adhesive; (o) indicates the shear force that was sustained. Fibrillar samples 1–3 are individual samples fabricated by the same methods. Bottom images: optical images showing the whole contact area after each simulated step (1 cm scale bars). (MS) Microspheres deposited on a glass substrate by fibrillar sample 1 at each step. The quantity of microspheres deposited on the glass decreases with increasing step number.

To quantify the self-cleaning capability of the adhesives, the shear adhesion strength was measured by applying a load parallel to the glass substrate during every simulated step as shown in Figure 3C. (The normal compressive load is zero during this phase of the testing cycle; this is not a friction test.) With no contamination, both fibrillar adhesives and PSAs could sustain a 4 N load parallel to a glass substrate (precleaned microscope slides, Fisher Scientific). (We limited the shear force to 4 N to prevent plastic deformation or tearing of the samples' thin backing.) After the samples were contaminated, the initial shear load tried was 0.2 N. This shear load was tested at every simulated step until the sample could sustain it (eight simulated steps for fibrillar adhesive sample 1). Once the sample could sustain this load, the shear load was increased by 0.1 N for the next simulated step. Following 30 successive simulated steps, fibrillar adhesive sample 1 could sustain a shear load of 1.0 N but did not show further improvement with five more simulated steps. This saturation is consistent with the quantity of microspheres deposited on the glass substrate after each step, as shown in the bottom three images in Figure 4. Initial contact steps left many

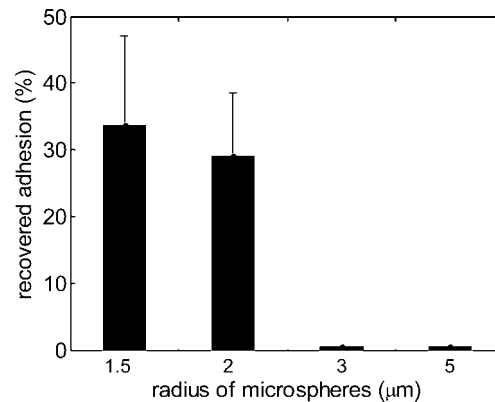


Figure 5. Cleaning performance by microsphere size. When the samples were contaminated with 1.5- and 2- μm -radius microspheres, the shear adhesive force recovered to 33 and 29%, respectively, of the clean value after 20–25 steps. For larger particles (3 and 5 μm), the adhesive force did not recover.

microspheres on the clean glass substrate, with diminishing particle removal after further steps. As expected, the PSA contaminated by microspheres did not recover any shear adhesion and could not sustain 0.05 N, even after 35 steps.

The synthetic fibrillar adhesives did not self-clean larger particles during contact. To observe the self-cleaning dependence on particle size, four differently sized polystyrene microspheres, 1.5, 2, 3 (also containing 12% 5 μm), and 5 μm in radius (Corpuscular Inc.), were used as dirt particles. Unlike gold microspheres, dry polystyrene microspheres contained lumps of microspheres. To obtain single-sized microspheres, we mixed dry polystyrene microspheres in isopropanol in about a 1:30 ratio. The mixture was ultrasonically agitated (2510 Branson) for 10 min to separate lumps. Then, several drops of microspheres in an isopropanol suspension were deposited on a clean glass slide and air dried. Air-dried polystyrene microspheres became approximately single-layered. The polystyrene microspheres were transferred to fibrillar adhesives by dragging adhesive samples on the glass slide covered with the single-layer microspheres. The shear adhesive strength of clean samples before being contaminated with polystyrene microspheres was 4 N. Prior to reuse, fibrillar samples were cleaned by removing clogged microspheres in an isopropanol bath with an ultrasonic cleaner (2510 Branson) for 2 min. After ultrasonic cleaning, samples could again hold 4 N of shear.

Contaminated samples with uniformly sized polystyrene microspheres were tested with the same methods for gold particles as described in Figure 4. After typically 20–25 simulated steps, samples contaminated with 1.5- μm -radius microspheres recovered about 34% (SD = 13%, three arrays, six measurements) of the shear force of uncontaminated samples, as shown in Figure 5. Samples contaminated with 2- μm -radius microspheres recovered about 29% of the shear force of uncontaminated samples (SD = 9%, three arrays, six measurements) after 20–25 steps. However, samples contaminated with 3- and 5- μm -radius particles could not sustain 0.2 N in shear (5% of the shear force of uncontaminated samples, three samples, six measurements) even after 25 steps.

The contact self-cleaning of the fibrillar adhesives demonstrated above is consistent with a greater affinity of the microspheres for the glass substrate than for the fibers as described for natural gecko setae.⁵ The self-cleaning of natural gecko setae⁵ was explained by comparing attraction forces and energies acting on a microsphere in contact with spatulae and a glass substrate. Hansen and Autumn⁵ argue that the small number of spatulae

contacting a spherical particle have less net adhesive force than particle adhesion to a flat substrate. We use a similar argument as with Hansen and Autumn⁵ for self-cleaning using the Johnson–Kendall–Roberts (JKR) contact model²⁹ and reported surface energies.^{30,31} Neglecting surface roughness, we can estimate the adhesion forces from the JKR model.²⁹ The sphere–glass pull-off force is

$$F_{sg} = \frac{3}{2}\pi R_s W_{sg}$$

and the sphere–fiber pull-off force is

$$F_{sf} = \frac{3}{2}\pi \frac{R_f R_s}{R_f + R_s} W_{sf}$$

with mean radius $R_s = 1.15 \mu\text{m}$ for gold microspheres (Alfa Aesar) and fiber radius $R_f = 0.3 \mu\text{m}$. The work of adhesion is estimated with

$$W_{sg} \approx 2\sqrt{\gamma_s \gamma_g}$$

and

$$W_{sf} \approx 2\sqrt{\gamma_s \gamma_f}$$

(ref 32) where the surface energy is $\gamma_g = 115\text{--}200 \text{ mJ/m}^2$ for SiO_2 ³⁰ and $\gamma_f = 30 \text{ mJ/m}^2$ for polypropylene.³¹ The ratio of pull-off forces is

$$N = \frac{F_{sg}}{F_{sf}} = \left(1 + \frac{R_s}{R_f}\right) \sqrt{\frac{\gamma_g}{\gamma_f}}$$

and contact with $N > 9$ fibers would be required to balance the microsphere–substrate contact. Considering an average fiber spacing of $1.5 \mu\text{m}$, the typical microsphere (mean radius $R_s = 1.15 \mu\text{m}$) will be in contact with one to four fibers (Figure 2B). Thus, the microspheres are preferentially attracted to the glass substrate instead of the fibrillar adhesive. Note that the ratio of pull-off forces is independent of γ_s . Although we have not tested other substrates, we predict contact self-cleaning for materials with small γ_f compared to γ_g .

Because the sphere–glass pull-off force F_{sg} is proportional to R_s whereas the total sphere–fiber pull-off force $N_f F_{sf}$ is approximately proportional to R_s^2 (N_f is the number of fibers in the projected area of a microsphere), larger particles will not self-clean. The SEM images in Figure 6 show that 1.5- (Figure 6A) and 5- μm -radius (Figure 6B) polystyrene microspheres (Corpuscular Inc.) remain in contact with fibers after 25 simulated steps. From Figure 6, a 1.5 μm polystyrene particle is in contact with one to four fibers whereas 5 μm particles are embedded among fibers, many of which are also in side contact with the microspheres. Note that side contact has much more contact area than tip contact, which makes large radius particle self-cleaning less likely.³³ From geometry, a 1.5- μm -radius microsphere comes into contact with an average of 3 fibers whereas a 5- μm -radius microsphere comes into contact with an average of 33 fibers. Hence, it is less energetically favorable to self-clean 5- μm -radius particles than smaller particles. The results of self-cleaning smaller particles and not self-cleaning larger particles support the model that fibrillar adhesives self-clean by unbalanced pull-off forces

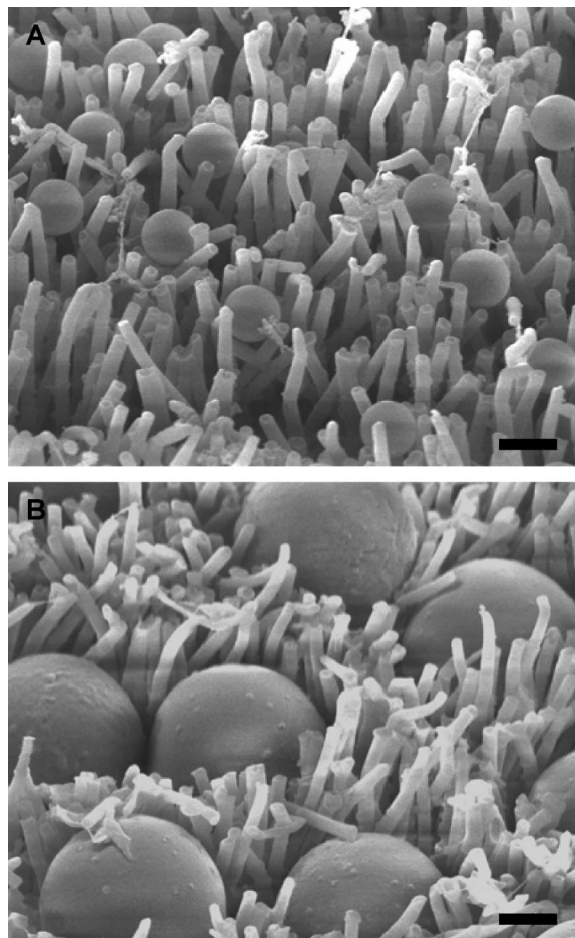


Figure 6. SEM images showing two differently sized microsphere particles remaining on the fibrillar adhesive after simulated steps. (A) The radius of the particles is $1.5 \mu\text{m}$. A $1.5 \mu\text{m}$ particle makes contact with one to four fibers. (B) The radius of the particles is $5 \mu\text{m}$. From the density of fibers and size of a particle, a $5 \mu\text{m}$ particle makes contact with 33 fibers. From the SEM image, the $5 \mu\text{m}$ particles are in side contact with fibers. Note that side contact has much more contact area than tip contact. The scale bars are $3 \mu\text{m}$.

on smooth surfaces. From the JKR pull-off model, we can roughly predict a critical particle size of $5.2 \mu\text{m}$ radius (with $R_f = 300 \text{ nm}$, $\gamma_g = 115 \text{ mJ/m}^2$, and $\gamma_f = 30 \text{ mJ/m}^2$). Particles larger than the critical particle size may not be self-cleaned. Experimentally, we found that particles with radius greater than $2 \mu\text{m}$ did not contact self-clean (Figure 5). The overestimation of the predicted critical particle size compared to $2 \mu\text{m}$ may be due to uncertainty in the tip shapes of fibers and possible side contact between fibers and spherical particles.

The dry contact self-cleaning of one microsphere is illustrated in Figure 7. Initially, the microsphere is in contact with fibers. When the fibrillar adhesive is preloaded, the microsphere makes contact with the flat glass substrate. During the simulated step, the microsphere may roll³⁴ or slide³⁵ as shown in Figure 7B, but displacement during a simulated step is quite small compared to the fiber array size, and hence the microsphere maintains contact with the substrate and fibers before detachment. During detachment, the microsphere is under tension between fibers and the substrate. At detachment, the microsphere is deposited on the glass substrate as a result of the greater affinity of the

(29) Johnson, K. L.; Kendall, K.; Roberts, A. D. *Proc. R. Soc. London, Ser. A* **1971**, *324*, 301.

(30) Yu, M.-F.; Kowalewski, T.; Ruoff, R. S. *Phys. Rev. Lett.* **2001**, *86*, 87.

(31) Novák, I. *J. Mater. Sci. Lett.* **1996**, *15*, 1137.

(32) Israelachvili, J. N. *Intermolecular and Surface Forces*, Academic Press: Oxford, U.K., 1991; pp 139–151.

(33) Majidi, C. S.; Groff, R. E.; Fearing, R. S. *J. Appl. Phys.* **2005**, *98*, 103521.

(34) Hui, C. Y.; Shen, L.; Jagota, A.; Autumn, K. *Mechanics of Anti-Fouling or Self-Cleaning in Gecko Setae*. In *Proceedings of the 29th Annual Meeting of The Adhesion Society*, 2006.

(35) Sitti, M. *IEEE-ASME Trans. Mech.* **2004**, *9*, 343.

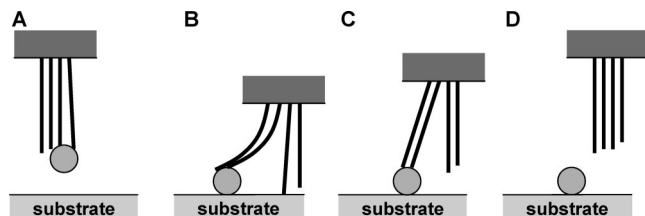


Figure 7. Illustration of dry self-cleaning. (A) Before contact. (B) During loading. A microsphere may roll or slide, but it is still in contact with the substrate and fibers. (C) During detachment. A microsphere is under tension between fibers and substrate. (D) After detachment, with a microsphere deposited on the substrate.

microsphere for the glass substrate than for the fibers. Thus, more fiber tips are exposed to the substrate in the next step, increasing adhesion.

Surface roughness may help self-cleaning³⁶ by catching particles during sliding, but under our experimental conditions (rms surface roughness of the glass slide scanned with an atomic force microscope (Metrology AFM, Molecular Imaging Inc.) is 3.3 nm) the surface roughness is about 1/1000 of the particle size.

The dry self-cleaning of the natural gecko setae⁵ and the synthetic fibrillar adhesive do not use water droplets, which are required for the wet self-cleaning (lotus effect) of nonadhesive surfaces. Although we report only the dry self-cleaning of the fibrillar adhesive in this letter, the superhydrophobic surface (water contact angles of 150–160°) of the fibrillar adhesive also shows almost complete wet self-cleaning with water droplets.

(36) Persson, B. N. J. *J. Adhes. Sci. Technol.* **2007**, *21*, 1145.

In conclusion, stiff polymer fibrillar adhesives showed self-cleaning properties with microspheres (radius $\leq 2.5 \mu\text{m}$), as samples recovered 25–33% of the original shear adhesion force after 30 simulated steps. In contrast, shear adhesion in gecko toes recovered 36% of the clean value after only eight steps using a larger particle size (radius $\leq 6 \mu\text{m}$),⁵ even though the contamination method and the simulated step protocol were not exactly the same. The higher efficiency of the natural gecko setae may be from the hierarchical structure of the gecko setae. The natural gecko's spatula tips may push off particles efficiently while switching back and forth between adhesive and nonadhesive states. Also, longer natural setae provide more space between them, thus there may be a higher probability for larger particles to be removed from spatula tips. Experiments with different sized polystyrene microspheres showed that the synthetic fibrillar adhesives did not self-clean larger particles, which is consistent with a JKR pull-off force model. In addition, the large embedded microspheres protrude above the fiber tips, preventing fibers from making contact with the substrate and thus preventing adhesion. We expect that as fabrication technology develops further, future hierarchical structured fibrillar adhesives will have thin, flat spatula tips and more space between fibers and hence will be able to self-clean a wider range of particle sizes with fewer steps as natural gecko setae do.

Acknowledgment. We thank Professor K. Komvopoulos, B. Bush, B. Schubert, and C. Majidi. This work was supported by NSF NIRT (no. EEC-034730).

LA8021485